EFFICIENT SINGLE IMAGE DEHAZING BY DARK CHANNEL PRIOR WITH DWT TECHNIQUE

B. Varshika[1], G. Harish babu[2]
1,2 Electronics and Communication Department, CVR College of Engineering, Hyderabad,Telengana,India

Abstract-The presence of haze inside the ecosystem degrades the great of photos captured by way of seen camera sensors. The removal of haze, known as dehazing, is typically carried out underneath the bodily degradation model, which necessitates a solution of an sick-posed inverse problem. To relieve the issue of the inverse problem, a novel previous known as dark channel prior (DCP) became these days proposed and has obtained a tremendous deal of attention. The DCP is derived from the feature of herbal outside pictures that the intensity price of at least one coloration channel inside a neighborhood window is close to zero. Based on the DCP, the dehazing is accomplished through 4 main steps: atmospheric slight estimation, transmission map estimation, transmission map refinement, and photograph reconstruction. This 4-step dehazing method makes it viable to provide a step-via-step method to the complex answer of the unwell-posed inverse hassle. This also permits us to shed mild at the systematic contributions of recent researches associated with the DCP for each step of the dehazing device. Our precise survey and experimental evaluation on DCP-based totally strategies will help readers recognize the effectiveness of the person step of the dehazing technique and will facilitate development of advanced dehazing algorithms channel previous, Dehazing, Image degradation, and Image recuperation..
Keywords: Dark channel prior

I.INTRODUCTION

Due to absorption and scattering through atmospheric debris in haze, out of doors photographs have horrible visibility below inclement climate. Poor visibility negatively impacts not handiest purchaser pictures but also computer vision applications for outside environments, which include item detection [1] and video surveillance [2]. Haze removal that is referred to as dehazing, is taken into consideration an important technique because haze-unfastened images are visually beautiful and may substantially improve the overall performance of computer vision obligations.

Methods offered in earlier studies had required multiple pictures to carry out dehazing. For instance, polarization-primarily based totally techniques [3–5] use the polarization property of scattered mild to restore the scene intensity facts from or greater pix fascinated approximately one-of-a-type tiers of polarization. Similarly, in [6, 7], multiple photographs of the same scene are captured beneath unique climate situations to be used as reference photographs with easy weather conditions. However, the ones techniques with more than one reference photos have catch 22 situation in on-line image dehazing.

packages [6, 7] and might need a completely unique imaging sensor [1–3]. This leads the researchers to awareness the dehazing approach with a single reference image. Single picture based totally absolutely techniques rely on the ordinary traits of haze-unfastened pics. Tan [8] proposed a method that takes into account the characteristic that a haze-loose picture has a better evaluation than a hazy photograph. By maximizing the neighborhood comparison of the input hazy photograph, it enhances the visibility however introduces blocking off artifacts round intensity discontinuities. Fattal [9] proposed a way that infers the medium transmission via estimating the albedo of the scene.

The underlying assumption is that the transmission and floor shading are regionally uncorrected, which does now not maintain beneath a dense haze. Observing the property of haze-unfastened out of doors pix, He [10] proposed a singular earlier—darkish channel in advance (DCP). The DCP is primarily based at the belongings of "dark pixels," that have a totally low depth in at least one shade channel, except for the sky vicinity. Owing to its effectiveness in dehazing, the majority of new dehazing strategies [10–36] have followed the DCP. The DCP-based absolutely dehazing strategies are composed of 4 foremost steps: atmospheric light estimation, transmission map estimation, transmission map refinement, and picture reconstruction. In this paper, we carry out an in-depth evaluation of the DCP-based totally strategies within the 4-step component of view.

We word that there are numerous evaluate papers on image dehazing or defogging [37–42]. In [37], 5 bodily model-primarily based completely dehazing algorithms are in evaluation. In [38, 39], severa enhancement-based and recovery based totally completely defogging techniques are investigated. In [40], fog removal algorithms that use intensity and former records are analyzed. In [41], a comparative examine at the 4 consultant dehazing techniques [4, 9, 10, 43] are performed. In [42], many visibility enhancement techniques evolved for homogeneous and heterogeneous fog are cited. To the high-quality of our expertise, our paper is the primary one dedicated to DCP-based absolutely strategies. This survey is expected to look at researchers' endeavors in the direction of enhancing the genuine DCP technique.

The rest of the paper is prepared as follows. In Section 1.2, the proper DCP-based totally dehazing technique is first reviewed. Section 1.Three affords an in-intensity survey of traditional DCP-based totally strategies. Section 1.Four discusses the overall

performance assessment methods for picture dehazing, and Section 1.5 concludes the paper.

II. LITERATURE SURVEY

1. E Kermani, D Asemani, A sturdy adaptive algorithm of moving object detection for video surveillance. EURASIP J. Image Video Process. 2014(27), 1–nine (2014).

In visible surveillance of each people and cars, a video movement is processed to symbolize the activities of interest thru the detection of shifting objects in every frame. The majority of mistakes in higher-stage duties consisting of monitoring are often because of faux detection. In this paper, a unique approach is delivered for the detection of transferring objects in surveillance packages which combines adaptive filtering approach with the Bayesian exchange detection set of policies. In proposed method, an adaptive shape first off detects the edges of motion objects. Then, Bayesian set of regulations corrects the form of detected items. The proposed method well-known extensive robustness in opposition to noise, shadows, illumination modifications, and repeated motions within the historical past in comparison to in advance works. In the proposed algorithm, no previous information about foreground and history is needed and the motion detection is completed in an adaptive scheme. Besides, it's miles established that the proposed algorithm is computationally efficient so that it can be effects applied for online surveillance structures similarly to comparable packages.

2. M Ozaki, K Kakimuma, M Hashimoto, K Takahashi, Laser-based totally pedestrian tracking in outside environments by means of multiple cell robots, in Proceedings of Annual Conference on IEEE Industrial Electronics Society 2011 (IECON, Melbourne, 2011), pp. 197–202

This paper provides an outdoors laser-based definitely pedestrian monitoring machine the use of a hard and fast of mobile robots positioned close to each exceptional. Each robotic detects pedestrians from its non-public laser take a look at photo the use

Ahmed Helmy et al.[8] proposed new algorithm for automatic test generation for multicast routing. They used the forward and backward search techniques to generate the test. of an occupancy-grid-primarily based technique, and the robot tracks the detected pedestrians thru Kalman filtering and international-nearest-neighbor (GNN)-based records affiliation. The tracking statistics is broadcast to a couple of robots via intercommunication and is mixed the use of the covariance intersection (CI) method. For pedestrian monitoring, every robot identifies its non-public posture the use of actual-time-kinematic GPS (RTK-GPS) and laser test matching. Using our cooperative monitoring method, all the robots proportion the tracking data with each exceptional; as a result, man or woman robots can continuously recognize pedestrians which might be invisible to every other robotic. The simulation and experimental results show that cooperating tracking offers the tracking normal performance higher than traditional person tracking does. Our tracking tool features in a decentralized way without any crucial server, and therefore, this gives a diploma of scalability and robustness that cannot be finished through way of conventional centralized architectures.

3. YY Schechnner, SG Narasimhan, SK Nayar, Polarization-based vision via haze. Appl. Optics 42(three), 511–525 (2003)

technique, but, stems from physics-based completely analysis that works below a wide variety of atmospheric and viewing situations, although the polarization is low. The method does no longer rely upon unique scattering models which includes Rayleigh scattering and does not depend upon the information of illumination suggestions. It may be used with as few as pics taken thru a polarizer at distinctive orientations. As a byproduct, the technique yields a ramification map of the scene, which permits scene rendering as if imaged from unique viewpoints. It moreover yields data about the atmospheric debris. We present experimental effects of entire dehazing of out of doors scenes, in a ways-from-ideal situations for polarization filtering. We obtain a fantastic improvement of scene assessment and correction of shade.

4. YY Schechnner, SG Narasimhan, Instant dehazing of images using polarization, in Proceedings of IEEE Computer Society Conference on Computer Vision and Pattern Recognition (CVPR, Kauai, 2001), pp. 25–332

We present an technique to without issues do away with the outcomes of haze from images. It is based totally mostly on the fact that usually air light scattered by way of the use of atmospheric particles is partially polarized. Polarization filtering by myself cannot put off the haze consequences, except in limited situations. Our technique, but, works below a extensive range of atmospheric and viewing conditions. We analyze the photo formation system, taking into consideration polarization results of atmospheric scattering. We then invert the procedure to allow the elimination of haze from photographs. The approach can be used with as few as pictures taken thru a polarizer at distinct orientations. This method works immediately, without counting on modifications of climate situations. We gift experimental results of entire dehazing in a long way from excellent situations for polarization filtering. We obtain a wonderful improvement of scene evaluation and correction of colour. As a byproduct, the technique additionally yields a range (intensity) map of the scene, and records approximately residences of the atmospheric debris.

III. EXISTING METHOD

3.1 Dark channel construction

Most traditional DCP-based totally dehazing strategies estimate the dark channel from the input hazy image I. In Eq. (4), the size of the close by patch Ω(x) is the handiest parameter that desires to be determined. Although the effect of the size of the nearby patch is massive, most traditional techniques truely use a community patch with a hard and fast length or do no longer specify the dimensions of the nearby patch. Table 2 indicates well known patch sizes used inside the previous techniques.

Figure 5a shows hazy pics. The pinnacle row in Fig. Five corresponds to a remote aerial photo with much less local texture and heavy haze. Therefore, a small local patch is sufficient which will estimate the dark channel, ensuing in a reduction within the DCP calculation time.

However,an picture that has complex nearby textures, as shown in the second row of Fig. 5, desires a larger neighborhood patch duration to exclude faux textures from the darkish channel. Note that the block-min way of Eq. (4) always decreases the apparent choice of the darkish channel as the scale of the patch will increase. Therefore, the minimal feasible patch period that doesn't produce fake textures within the darkish channel desires to be placed for every hazy image through way of thinking about software-primarily based photograph neighborhood information.

Apart from the aforementioned preferred technique for the dark channel estimation, Zhang [23] replaced the minimum operator by manner of the median operator as follows:

$$\boldsymbol{I^{\mathbf{dark}}(x) = \underset{y\epsilon\Omega(x)}{\mathbf{median}} \left(\min_{c\in\{r,g,b\}} I^c(y) \right).} \qquad (1)$$

As a end result of the median operation, the dark channels emerge as tons much less blurry, as proven in Fig. 6. However, the median operator is computationally extra complicated than the minimal operator. Moreover, the median-based totally absolutely approach is of Fig. 6, less bodily meaningful due to the fact the belief of the DCP will become deteriorated. As shown inside the 2d row dense picture textures continue to be seen for the dark channel, even supposing a massive patch duration of 15 × 15 is used. For the sake of the visibility enhancement of hazy pics, however, the median clear out is in particular effective because it does no longer require complicated publish-processing, this is crucial for clean and blurry dark channels which are acquired by way of the minimum operator.

3.2 Atmospheric light estimation

The majority of traditional DCP-primarily based dehazing strategies estimate A as defined in Section 1.2.Three. In [19, 20], the pixel with the very excellent dark channel price is used right now as follows:

$$\mathbf{A = \ I\left(argmax_x\left(I^{dark}(x)\right)\right).} \qquad (2)$$

However, the above approach can incorrectly select the pixel when the scene consists of first rate gadgets. Instead, pixels with a top p% darkish channel values are decided on due to the fact the maximum haze-opaque pixels, and the best with the very pleasant depth is used to estimate A. This stays one parameter p inside the estimation of A, which is empirically set as zero.1 [10–15] or 0.2 [16].

In [21], to explicitly exclude bright objects from the estimation of A, the close by entropy is measured as

$$\mathbf{E(x) = \sum_{i=0}^{N} (p_x(i) * log_2(p_x(i)),} \qquad (3)$$

Where p x(i) represents the possibility of a pixel cost i within the nearby patch centered at x, and N represents themaximum pixel fee. The community entropy price is low for areas with smooth versions, which surprisingly likely correspond to haze-opaque areas. Therefore, the pixel with the lowest entropy price is used to reap A most of the maximum p% pixels inside the darkish channel (p = 0.1 [21]).

Table 3 lists the traditional techniques which is probably used to estimate atmospheric mild. To quantitatively take a look at atmospheric slight estimation techniques, we used the foggy street image database (FRIDA) [38] which incorporates pairs of synthetic color and intensity photos. For a given depth photograph and β, the floor-fact transmission map can be constructed as t(x) = e− βd(x). The hazy photo I is

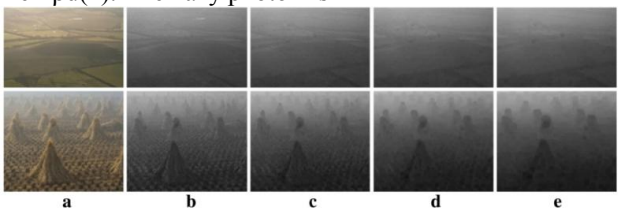

Fig. 5 Dark channels of various patch size obtained by Eq. (4). a Hazy image. Dark channels obtained by Eq. (4) with the patch size of (b) 3 × 3, (c) 7 × 7, (d) 11 × 11, and (e) 15 × 15.

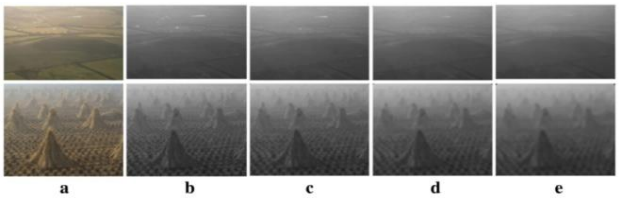

Fig. 6 Dark channels of diverse patch duration obtained through Eq. (12). A Hazy photographs. Dark channels received via Eq. (12) with the patch period of (b) 3 × (c) 7 × 7, (d) eleven × eleven, and (e) 15 × 15.

Then received as Eq. (6) with the aid of using the atmospheric mild A. Therefore, a variety of hazy photographs may be generated by using the usage of converting β (haze density) and A (global lightness).

Figure 7 suggests the common root-advise-square errors (RMSE) between the floor-fact and estimated atmospheric lights for the 66 test images in the FRIDA. The RMSE is acquired as

$$\boldsymbol{RMSE} = \sqrt{\frac{1}{3}((\hat{A}_R - A_R^*)^2 + (\hat{A}_G - A_G^*)^2 + (\hat{A}_B - A_B^*)^2)},$$

Where ,A^*=(A_R^* A_G^* A_B^*) and Aˆ=[Aˆ_R Aˆ_G Aˆ_B]represent the floor-reality and predicted atmospheric lighting, respectively. Since the candidate pixels for the atmospheric mild estimation are acquired from the darkish channel, the local patch length also plays an critical function within the accuracy of the estimation. When a small patch length is used, as confirmed in Fig. 8b, the pixels for greasy gadgets are taken into consideration as candidate pixels, yielding faulty A estimates. The use of a large patch length can save you selecting such pixels, as established in Fig. 8c. The quantitative evaluation end result as proven in Fig. 7a moreover supports our remark. The accuracy is instead insensitive to p while a big 32 × 32 patch is used. Therefore, a massive patch size (e.g., 32 × 32) with p = zero~0.Four % is effective fine whilst the into consideration. One sensible answer that takes under consideration the accuracy of each the dark channel and the atmospheric mild entails the usage of one of a kind patch sizes to estimate the dark channel estimation and atmospheric mild [26]. When the neighborhood entropy, as in Eq. (15), is used to prevent pixels of small vivid

gadgets from being decided on, the estimation accuracy of the atmospheric light improves, as tested in Fig. 7b [21]. The estimation accuracy continues to be pleasant for the most important patch length of 32 × 32 and is less touchy to the p value due to the robustness of candidate pixel choice.

3.3 Transmission map estimation

The transmission map ~t x ð Þ fined in Eq. (9) is obtained from the DCP. If the DCP is not exploited, Eq. (nine) may be rewritten as

$$\tilde{t}(x) = 1 - \min_{\gamma\epsilon\Omega(x)}(\min_{c}\frac{I^c(\gamma)}{A^c}) + \tilde{t}(x)\min_{\gamma\epsilon\Omega(x)}(\min_{c}\frac{J^c(\gamma)}{A^c}). \quad (5)$$

As we determined in Section 1.2.2, the pixel price of the darkish channel, J dark(x), is rather probable zero, and so is (J/A)darkish(x). However, if (J/A)darkish(x) is not close to 0, the transmission map received as Eq. (nine) can be beneath-expected because the great offset in Eq. (16) is usually omitted [28].

In the actual DCP-based totally dehazing technique, it is stated that the photo may additionally moreover accuracy of the atmospheric slight estimation is taken appearance unnatural if the haze is removed very well [10]. A constant ω (zero < ω < 1) is for that reason used to preserve a small quantity of haze:

$$\tilde{t}(x) = 1 - \omega\min_{\gamma\epsilon\Omega(x)}(\min_{c}\frac{I^c(\gamma)}{A^c}). \quad (6)$$

However, we consider that a better visibility in the dehazed picture can be completed with Eq. (17) because of the reality we inadvertently capture up on the beneath-estimation of ~t x ð Þ via manner of multiplying ω.

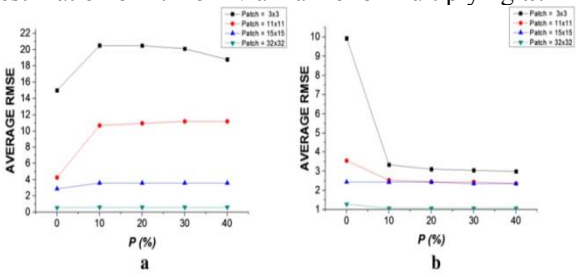

Fig. 7 The common RMSE between the ground-fact (A* = [220,235,254]) and the expected atmospheric slight. The atmospheric light is anticipated from pixels with the highest p% dark channel values. Among the p% pixels, the pixel with (a) the very exceptional depth or (b) the bottom entropy price is used to estimate the atmospheric moderate. Sixty-six take a look at pics from the FRIDA had been used.

Figur.9 shows that the transmission map is indeed underneath-anticipated while ~t is obtained as Eq. (9). The recommend values of the ground-reality transmission maps, as shown in Fig. 9b, are zero.5616 and zero.6365, respectively. However, the advocate values for the predicted transmission maps, as proven in Fig. 9c, are received as 0.5125 and 0.6086, respectively. When the transmission map is obtained as Eq. (17) by using the use of ω = 0.Nine, the beneath-estimation of the transmission map is substantially reduced, as proven in Fig. 10a, c, wherein the mean values are obtained as zero.5225 and zero.6058, respectively.

Xu et al. [14] explicitly addressed the aforementioned beneath-estimation problem of the transmission map and

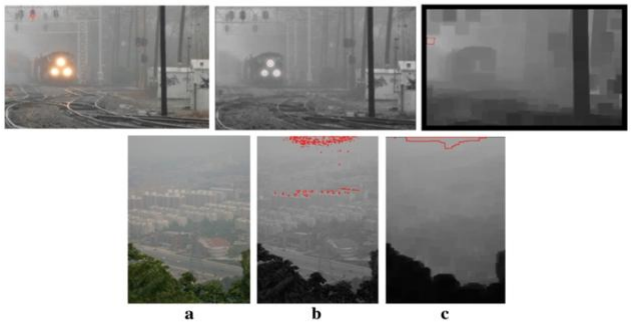

Fig.8 Atmospheric mild estimation. A Hazy picture. The pixels within the dark channel which can be used to estimate the atmospheric mild while the scale of Ω is (b) 3 × 3 and (c) 32 × 32

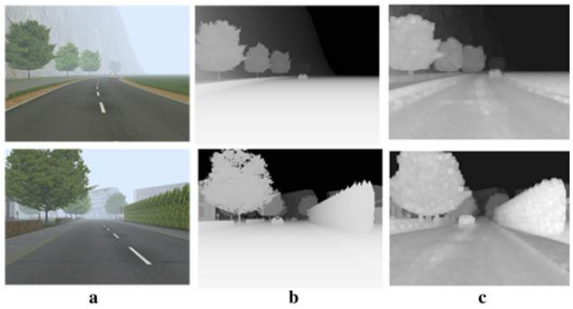

Fig.9 Hazy photos and floor-fact and expected transmission maps from the FRIDA [46]. A Hazy snap shots. B Ground-truth transmission maps, wherein A =[220,235,254] and β = zero.01. C Transmission maps received as Eq. (9).

For visualization, transmission values are accelerated by using 255 Simply brought a high-quality cost ρ ∈ [0.08, 0.25] to the transmission map:

$$\tilde{t}(x) = 1 - \min_{\gamma\epsilon\Omega(x)}(\min_{c}\frac{I^c(\gamma)}{A^c}) + \rho. \quad (7)$$

Figure 10b, d shows the anticipated transmission maps at the same time as ρ = 0.08 is introduced, in which the mean values are received as zero.5494 and 0.6431, respectively. The addition of ρ also plays a similar function of t0 in Eq. (11), making the minimal fee of the transmission map be ρ. The below-estimation may be in element solved by way of using Eq. (17) or (18); but, the values of ω and ρ want to be cautiously selected. To this forestall, we measured the RMSE values some of the floor-fact and predicted transmission maps for unique ω and ρ values through the use of 66 synthetic check images from the FRIDA. Figure 11a, b shows that ω around zero. Nine and ρ round zero.12 are effective. An adaptive scheme additionally needs to be developed for a higher compensation of the below-estimation.

IV. BILATERAL FILTER OUT

The bilateral clear out is a widely used aspect-preserving smoothing filter out. It uses weighted neighboring pixel values with the spatial and variety distances as follows:

$$\hat{t}(x) = \frac{1}{\sum_{y\epsilon\Omega(x)} G_\delta(||x-y||)\, G_\delta(|I(x)-I(y)|)} \cdot \sum_{y\epsilon\Omega(x)} G_\delta(||x-y||)\, G_\delta(|I(x)-I(y)|)\hat{t}(y), \quad (8)$$

Where Gσs and Gσr constitute the spatial and variety kernels with the equal vintage deviations σ s and σr, respectively. Since the neighboring pixels which have the identical pixel

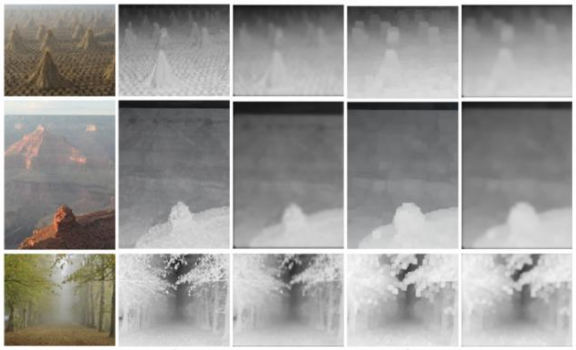

Fig. 12 The end result of the Gaussian clean out. A Hazy photos. B Transmission map received using the nearby patch with the scale three × three. C Gaussian filtered transmission map the usage of σs = five. D Transmission map obtained the use of the neighborhood patch with the size 15 × 15.

E Gaussian filtered transmission map the usage of σs = five fee with the middle pixel are notably weighted, edges in ~t can be preserved while smoothing noisy regions in ~t . The bilateral-filtered transmission maps as shown in Fig. 14 tend to expose off sharper info than the Gaussian filtered transmission maps as shown in Fig. 12.

We also evaluated the quantitative performance of the bilateral clear out as demonstrated in Fig. 15 using the same experimental circumstance of Fig. 14. σs is ready as 15 and the performance dependency on σr is excellent investigated. The consequences illustrate that the bilateral clear out isn't always very powerful in phrases of the quantitative performance and tends to growth the RMSE whilst the same old deviation of the variety kernel will increase

Proposed method :

Introduction to the Discrete Wavelet Transform (DWT)

Defination of DWT

In numerical analysis and functional analysis, a discrete wavelet transform (DWT) is any wavelet transform for which the wavelets are discretely sampled. As with other wavelet transforms, a key advantage it has over Fourier transforms is temporal resolution: it captures both frequency and location information (location in time).

Discrete Wavelet Transform

The wavelet transform has gained widespread acceptance in signal processing and image compression. Recently the JPEG committee has released its new image coding standard, JPEG-2000, which been based upon DWT. Wavelet transform, decomposes a signal into a set of basis functions. These basis functions are called wavelets. Wavelets are obtained from a single prototype wavelet called mother wavelet by dilations and shifting [8]. The DWT has been introduced as a highly efficient and flexible method for sub band decomposition of signals. The 2DDWT is nowadays established as a key operation in image processing .It is multi-resolution analysis and it decomposes images into wavelet coefficients and scaling function. In Discrete Wavelet Transform, signal energy concentrates to specific wavelet coefficients. This characteristic is useful for compressing images [9].

Wavelets convert the image into a series of wavelets that can be stored more efficiently than pixel blocks. Wavelets have rough edges; they are able to render pictures better by eliminating the ―blockiness‖. In DWT, a timescale representation of the digital signal is obtained using digital filtering techniques.

V.EXPERIMENTAL RESULTS

By using dark channel prior technique and bilateral filter we got less PSNR values so we used DWT technique for high PSNR values The below results are obtained using dark channel prior ,Bilateral filter and DWT technique

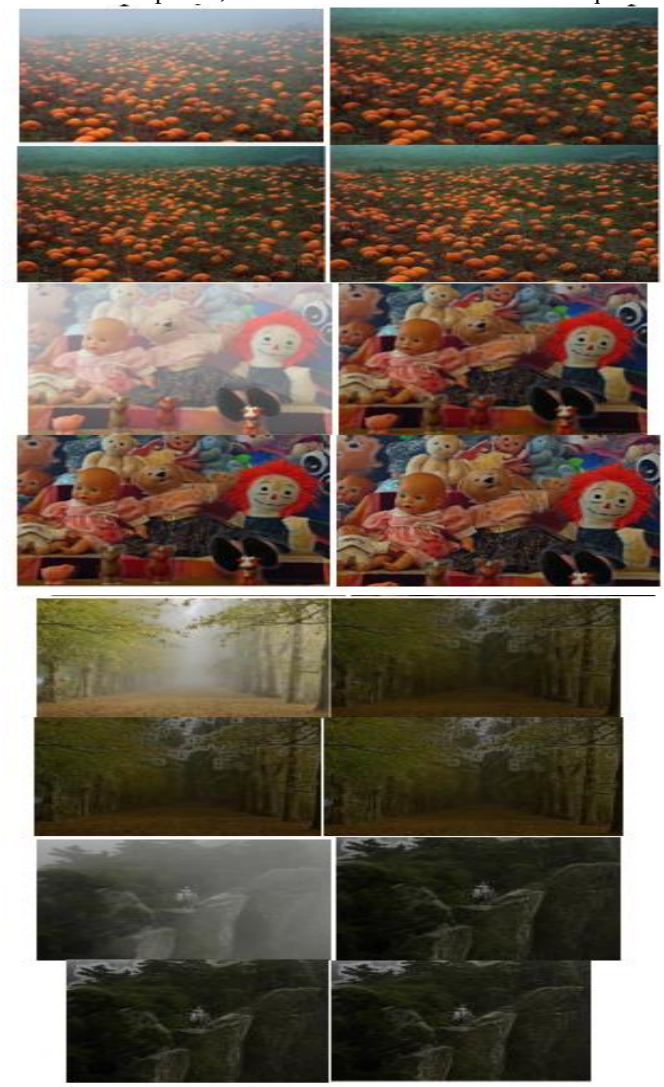

a) Input image, b) Dehazed image c) Dcp with bilateral filter d) DCP +bilateral+DWT

PARAMETERS;

S.no.	Dark Channel Prior			Bilateral filter			Discrete Wavelet Transform		
	MSE	RMSE	PSNR	MSE	RMSE	PSNR	MSE	RMSE	PSNR
1	0.8518	0.9229	3.1158	0.2381	0.40	4.7006	0.1934	0.439	51.9508
2	0.5098	0.7140	22.8437	0.2075	0.4556	41.3167	0.0634	0.2518	64.5150
3	0.4563	0.6755	37.1509	0.2708	0.5272	48.1709	0.0646	0.2542	65.1839
4	0.3253	0.5703	2.6929	0.4497	0.6706	40.3986	0.0321	0.1742	61.1385
5	0.8404	0.9167	32.5942	0.2695	0.5191	40.7162	0.1414	0.3761	60.0112

Quantitative Evaluation of PSNR and MSE

PSNR:

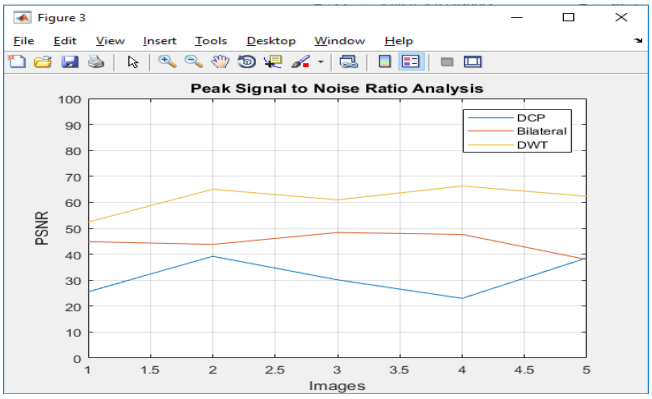

PSNR Comparison using different refinement methods This graph represents PSNR comparison between different refinement methods using DCP, Bilateral filter and DWT technique. On the basis of graph, it can be said that refinement using DWT has better PSNR value when compared with the other two.

Mean Square Error (MSE)

Mean square Error is another form of error measurement method that is widely used to assess the distinctions between the estimator's expected value and the real value. It assesses the magnitude of the mistake. It is a ideal precision metric that is used for a definite variable to execute the distinctions of forecast errors from the various estimators.

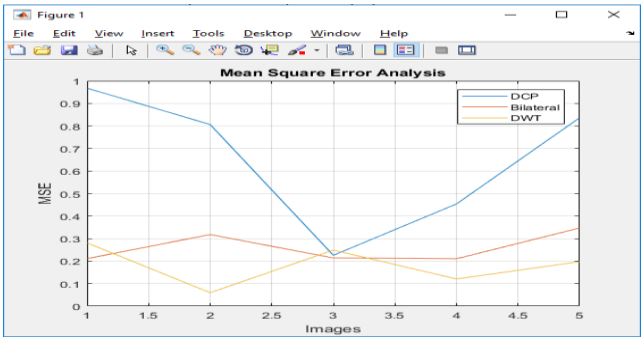

MSE Comparision Using Different Refinement Methodsrepresents MSE comparison between different refinement methods using DCP and bilateral filter and DWT technique. On the basis of graph, it can be said that refinement using DCP and bilateral filter has least MSE value.

VI CONCLUSION

In this paper, we carried out an in-depth observe on one of the most successful dehazing algorithms: the DCP-based totally picture dehazing set of guidelines. Considering the four most important steps of the DCP-based image dehazing, which is probably atmospheric mild estimation, transmission map estimation, transmission map refinement, and picture reconstruction, we categorized contemporary research articles associated with the DCP consistent with the ones 4 steps and performed a step-by step assessment of conventional techniques. Moreover, the conventional techniques evolved for evaluating the general overall performance of image de hazing had been moreover summarized and mentioned. We agree with that our genuine survey and experimental evaluation will assist readers understand the DCP based de hazing techniques and could facilitate development of advanced dehazing

REFERENCES

[1] E Kermani, D Asemani, A sturdy adaptive set of rules of shifting object detection for video surveillance. EURASIP J. Image Video Process. 2014(27), 1–9 (2014)

[2] M Ozaki, K Kakimuma, M Hashimoto, K Takahashi, Laser-based completely pedestrian monitoring in outdoor environments through multiple mobile robots, in Proceedings of Annual Conference on IEEE Industrial Electronics Society 2011 (IECON, Melbourne, 2011), pp. 197–202

[3] YY Schechnner, SG Narasimhan, SK Nayar, Polarization-based totally vision via haze. Appl. Optics 40 two(three), 511–525 (2003)

[4] YY Schechnner, SG Narasimhan, Instant dehazing of pics the use of polarization, in Proceedings of IEEE Computer Society Conference on Computer Vision and Pattern Recognition (CVPR, Kauai, 2001), pp. 25–332

[5] S Shwartz, E Namer, YY Schechner, Blind haze separation, in Proceedings of IEEE Computer Society Conference on Computer Vision and Pattern Recognition (CVPR) (CVPR, Anchorage, 2006), pp. 1984–1991

[6] SG Narasimhan, SK Nayar, Contrast restoration of climate degraded snap shots. IEEE Trans. Pattern Anal. Mach. Intell. 25(6), 713–724 (2003)

[7] SK Nayar, SG Narasimhan, Vision in awful climate, in Proceedings of the seventh IEEE International Conference on Computer Vision (ICCV, Kerkyra, 1999), pp. 820–827

[8] RT Tan, Visibility in terrible climate from a unmarried picture, in Proceedings of IEEE Computer Society Conference on Computer Vision and Pattern Recognition (CVPR, Anchorage, 2008), pp. 1–8

[9] R Fattal, Single photo dehazing. ACM Trans. Graph. Seventy two(three), seventy two:1-seventy two:nine (2008)

[10] K He, J Sun, X Tang, Proceedings of IEEE Computer Society Conference on Computer Vision and Pattern Recognition (CVPR, Miami, 2009), pp. 1956–1963.